Modulation of the Spontaneous Curvature and Bending Rigidity of Lipid Membranes by Interfacially Adsorbed Amphipathic Peptides

Assaf Zemel,*,† Avinoam Ben-Shaul,† and Sylvio May‡

Department of Physical Chemistry and the Fritz Haber Research Center, The Hebrew University, Jerusalem 91904, Israel, and Department of Physics, North Dakota State University, Fargo, North Dakota 58105-5566

Received: November 22, 2007; Revised Manuscript Received: February 20, 2008

Amphipathic α-helical peptides are often ascribed an ability to induce curvature stress in lipid membranes. This may lead directly to a bending deformation of the host membrane, or it may promote the formation of defects that involve highly curved lipid layers present in membrane pores, fusion intermediates, and solubilized peptide−micelle complexes. The driving force is the same in all cases: peptides induce a spontaneous curvature in the host lipid layer, the sign of which depends sensitively on the peptide's structural properties. We provide a quantitative account for this observation on the basis of a molecular-level method. To this end, we consider a lipid membrane with peptides interfacially adsorbed onto one leaflet at high peptide-to-lipid ratio. The peptides are modeled generically as rigid cylinders that interact with the host membrane through a perturbation of the conformational properties of the lipid chains. Through the use of a molecular-level chain packing theory, we calculate the elastic properties, that is, the spontaneous curvature and bending stiffness, of the peptide-decorated lipid membrane as a function of the peptide's insertion depth. We find a positive spontaneous curvature (preferred bending of the membrane away from the peptide) for small penetration depths of the peptide. At a penetration depth roughly equal to half-insertion into the hydrocarbon core, the spontaneous curvature changes sign, implying negative spontaneous curvature (preferred bending of the membrane toward the peptide) for large penetration depths. Despite thinning of the membrane upon peptide insertion, we find an increase in the bending stiffness. We discuss these findings in terms of how the peptide induces elastic stress.

1. Introduction

Modulating the curvature of a lipid membrane is a central step in a number of cellular processes such as vesicle trafficking, budding, fusion, drug and virus entry, and cellular defense. Cells use different mechanisms to modulate the curvature of the lipid membrane.[1–3] These include active forces that are generated by the cytoskeleton, assembly of curvature-generating membrane proteins to form a coating layer around the membrane, and incorporation of short, membrane-active peptides into the membrane. Much experimental and theoretical effort has been devoted to this latter mechanism and in particular, to the study of amphipathic α-helical peptides.[4,5] These peptides are often found as individual molecules with a designated biological function and as structural components in globular proteins. For example, the immune system of virtually all life forms includes a group of cytolytic peptides whose target is the lipid membrane. The adsorption of these amphipathic peptides on the host cell membrane leads to pore formation and to complete rupture at a sufficiently high peptide-to-lipid ratio.[6] Another relevant example concerns the amphipathic α-helical segments of water-soluble proteins called apolipoproteins;[4,7] these proteins are responsible for the transfer of lipids and cholesterol in the blood. The amphipathic helical segments of apolipoproteins are used to wrap around a bunch of lipid molecules and to solubilize them in the form of discoidal lipid complexes called lipoproteins. Amphipathic helices are also common constituents in many membrane proteins, often playing an important role in the interaction of the protein with the membrane and in particular cases in changing the local membrane curvature.[1,8,9] In addition to pore formation and solubilization of lipids, amphipathic peptides were shown to induce a variety of other effects in membranes. These include, variations in the shape of vesicles, fusion of membranes, tubulation, and modulation of the structure and stability of lipid phases.[1,5,10–13]

The distinctive structural characteristic of amphipathic helical peptides is the division of their cylindrical envelope along their main axis into complementary, hydrophobic, and hydrophilic regions. A common property of many amphipathic peptides is their strong affinity to the lipid membrane; this property is primarily, although not exclusively, due to the hydrophobic effect.[14] Consistent with their molecular structure amphipathic peptides often bind the membrane at the hydrocarbon−water interface with their hydrophobic sector dipping into the hydrocarbon region of the membrane.[6,15,16] This interfacial location of amphipathic peptides is unique in that it produces an *asymmetric perturbation* in the two lipid leaflets of the bilayer. This asymmetry induces an elastic curvature stress that is thought to provide a major driving force for the modulation of membrane shape.[4,5] Indeed, membrane pores, solubilized micelles, and fusion intermediates typically involve the formation of spatially confined and highly bent lipid monolayers with radii of curvature comparable to the length of a single lipid molecule.

* To whom correspondence should be addressed. Present address: Department of Neurobiology, Physiology, and Behavior, University of California at Davis, Davis, CA 95616

† The Hebrew University.

‡ North Dakota State University.

10.1021/jp711107y CCC: $40.75
Published on Web 05/14/2008

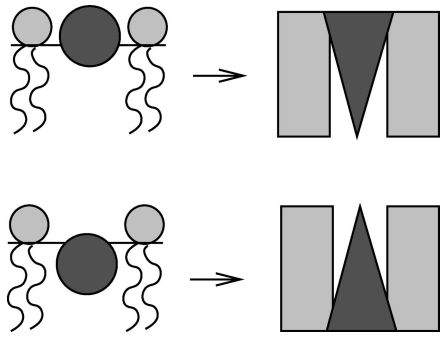

Figure 1. Interfacially adsorbed amphipathic α-helical peptides induce curvature stress in a lipid membrane. The peptides (illustrated in the left diagrams as dark-shaded circles, representing cross-sections along their long axis) penetrate partially into the hydrocarbon core of the host membrane (two lipid molecules are shown schematically) and thus perturb the lipid chain region. Displayed are two cases: small insertion depth (top left) and deep insertion (bottom left) of the peptide. Depending on the insertion depth, the peptide acts effectively like a wedge (top right) or like an inverted wedge (bottom right), imposing a curvature stress and thus driving the lipid layer to bend away from or towards the peptide.

The influence of interfacially adsorbed amphipathic peptides on a lipid membrane appears to follow a characteristic structural pattern.[4,17] That is, peptides with a number of similar structural properties are often found to exhibit similar biological activity. Of particular relevance is the polar angle, α, which separates the hydrophobic and hydrophilic sectors of the helix and (among other factors) dictates the penetration depth of the peptide into the membrane.[15,18] In accordance with the classification scheme introduced by Segrest et al.,[17] peptide segments of apolipoproteins and their synthetic analogs belong to class A. These peptides typically have a wide polar angle $\alpha > 180°$. In contrast, (lytic) antimicrobial peptides and their analogs belong to class L; these peptides typically, although not always, have a narrow polar angle, $\alpha < 180°$. Interestingly, class A and class L peptides exhibit reciprocal effects on membranes.[19,20] Class A peptides were shown to induce a positive curvature stress in membranes (i.e., promoting a bending of the peptide-containing monolayer away from the peptides), whereas class L peptides induced a negative curvature stress. These conclusions are based on measurements of the peptide-induced shifts of the bilayer (L_α) to inverse hexagonal (H_{II}) phase transition temperature. Another property that was attributed to the opposite curvature stress imposed by class A and class L peptides was their synergistic effect with respect to bilayer stability. When adsorbed on a bilayer formed from (frustrated) monolayers with negative spontaneous curvature, class A peptides stabilize the membrane with respect to permeabilization by class L peptides.[21] A rationale for the reciprocal effects of class A and class L peptides on a lipid membrane is provided by the different effective molecular shapes of the membrane-inserted peptides,[19] acting as wedges or inverted wedges,[2,19,22] respectively, and thus promoting positive or negative membrane curvature. Figure 1 illustrates the underlying concept of molecular shape;[19] most lipid molecules preferentially adopt a cylinder-like shape whereas the inserted peptide acts effectively as a wedge or an inverted wedge, depending on the insertion depth and other factors. Note that the representation of peptides and lipids as wedges and cylinders provides at best a conceptual framework. It does not quantify the energy basis of peptide-induced membrane bending. Calculation of the curvature elastic properties of a peptide-decorated membrane requires a molecular model. This is the subject of the present work.

The curvature elastic properties of a lipid membrane are generally and conveniently expressed in terms of the spontaneous curvature, c_0, and bending rigidity, κ, appearing in the familiar Helfrich curvature free energy.[23] (An additional material constant, the Gaussian modulus,[23] will be ignored here; see the discussion below.) These two material parameters characterize the preferred curvature of a lipid membrane and its resistance with respect to a bending deformation, respectively. They also suffice to characterize the "frustration energy" of a flat membrane whose two individual monolayers have a nonvanishing spontaneous curvature.[24] Both c_0 and κ depend on the type of lipids comprising the membrane. We obviously expect that interfacially adsorbed peptides also will modify the elastic characteristics of the host membrane.

In this paper, we present a molecular level theory that allows us to estimate the effects of interfacially adsorbed peptides on the elastic characteristics of the membrane, namely, the bending stiffness, κ, and the spontaneous curvature, c_0. Our focus here is on the generic effects resulting from the unavoidable perturbation of the lipid chain region by the peptides. This perturbation affects the conformational space of the lipid chains and as we shall see has a substantial effect on the elastic characteristics of the membrane. The contribution of the conformational statistics of the lipid chains to the overall elasticity of the membrane is well known both experimentally and theoretically.[25] We note that in general κ and c_0 may reflect additional interactions between the peptides and the membrane and among the peptides and the lipids themselves. These include nonspecific electrostatic and excluded volume interactions as well as specific interactions, such as salt-bridges and hydrogen bonds. Furthermore, the flexibility of the peptides (particularly short ones) and their ability to fluctuate in the membrane may also have an effect on the observed elastic properties. These effects require additional assumptions and approximations about the nature of the peptides and the membrane (see below) and are outside the scope of the present work.

To account for the effects of interfacially bound peptides on the hydrocarbon core of the membrane, we use a molecular level theory of lipid chain packing in membranes. The conformational free energy of the lipid chains in the membrane and its modification in the presence of the peptides is calculated on a mean-field level by generating all possible lipid chain conformations (see details in the section entitled Model) and evaluating their corresponding thermal (Boltzmann) weight. This approach has often been implemented to study the structural and energetic characteristics of the lipid tails in various lipid systems including spherical and cylindrical micelles, monolayers, bilayers, as well as other nonbilayer phases.[25] It has also been used to treat lipid−protein systems including transmembrane as well as interfacially adsorbed pepetides.[18,25–28] Among its applications was also the calculation of the curvature elastic properties of symmetric protein-free membranes.[29] This study provided a molecular-level explanation for the dependence of the membrane-bending stiffness on various lipid properties such as the lipid chain length and the lipid composition.

In this paper, we extend this approach to estimate the modulation of the curvature elastic properties of lipid membranes by interfacially adsorbed α-helical peptides. Our model predicts that such peptides (i) rigidify the membrane, and (ii) induce a spontaneous curvature that changes sign from positive to negative as the peptide inserts deeper into the membrane. These results are consistent with available experimental observations and provide a quantitative energetic basis to the reciprocal wedge hypothesis that was suggested to explain the

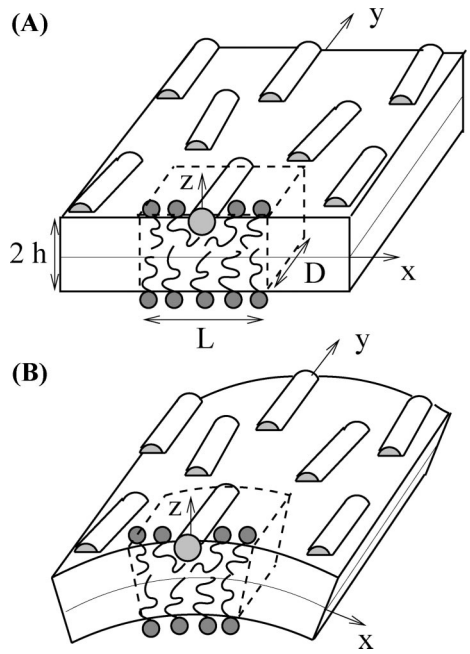

Figure 2. Schematic illustration of a peptide-decorated lipid membrane in flat (A) and curved (B) geometries. Peptides are adsorbed on one membrane leaflet only. Because of their high density they are oriented (at least locally) along a common axis (here, the *y*-axis). The broken lines indicate a unit cell (of dimensions $L \times D \times 2h$). Each unit cell contains a single peptide (of length D) and a fixed number, N, of lipid chains. The thickness of the membrane's hydrophobic region is $2h$; the (average) interhelical distance, L, determines the lateral extension of the unit cell along the *x*-axis.

different effects of class A and class L peptides on membranes. In addition, to the best of our knowledge this is the first modeling study that predicts the curvature elastic properties of a peptide−membrane system on the basis of a molecular-level model.

2. Model

We consider an initially flat lipid bilayer with amphipathic, α-helical, peptides adsorbed onto one of its monolayers, as schematically displayed in Figure 2A. Despite the possibility of an oblique orientation[30,31] we will only be concerned with the case of the peptide's long axis being parallel to the membrane surface. Ignoring all atomic details, we model the adsorbed peptides as rigid cylinders of length D and radius R. Clearly, the presence of the peptides affects the packing properties of the lipid chains by virtue of penetrating into the hydrocarbon core of the membrane. The chain packing approach described below allows us to predict the degree of perturbation and the corresponding cost in free energy.

Experiments are often carried out at high peptide concentration[32–34] where the average interhelical distance, L, between the peptides falls below D. In this concentration regime, excluded volume interactions tend to align the peptides in parallel to a common axis (for example, the *y*-axis of the Cartesian coordinate system in Figure 2), like in a two-dimensional nematic phase. In this case, it is appropriate to describe the energetics of the peptide-decorated membrane using a cell model.[18] Each cell contains one peptide and N lipids where $1/N$ reflects the experimentally controllable peptide-to-lipid ratio. The cell model assumes that the packing properties of the lipids depend only on their distance from the peptide along the *x*-axis but are invariant along the *y*-axis. Adopting the cell model we thus neglect modifications in the lipid chain packing at the peptide ends. These "end effects" are of minor importance as long as $D \gg R$.

In addition, as in previous work[18] we assume that the membrane is uniformly thick, that is, everywhere within the *x*, *y*-plane the thickness of the hydrocarbon core is $2h$; see Figure 2A. In this approximation, we ignore possible local variations in membrane thickness. Again, this assumption is appropriate for high peptide concentrations where L is not larger than the typical decay length for the spatial membrane relaxation.[35] It should be stressed that while we impose a uniform membrane thickness, $2h$, its magnitude is allowed to adjust upon peptide insertion as well as a function of peptide concentration.

Suppose the membrane is bent along the *x*-axis, as is schematically illustrated in Figure 2B. The corresponding dependence of F, the free energy per unit cell (having cross-sectional area $A_0 = LD$), on curvature, c, can be expressed as $F/A_0 = (\kappa/2)(c-c_0)^2$. Hence, if $F(c)$ is known we can calculate the spontaneous curvature c_0 and the bending modulus κ through

$$\kappa c_0 = -\frac{1}{A_0}\left(\frac{\partial F}{\partial c}\right)_{c=0} \qquad \kappa = \frac{1}{A_0}\left(\frac{\partial^2 F}{\partial c^2}\right)_{c=0} \tag{1}$$

At moderate curvature changes where the quadratic expansion is applicable, the derivatives of F can be evaluated at any curvature to obtain equivalent expressions for κ and c_0. Taking the derivatives at $c = 0$ is a suitable choice for the present system because, as we shall see below, membrane-inserted peptides are able to induce both positive and negative curvatures.

Assuming strong hydrophobic interaction between the membrane and the peptides, we need not consider a bending deformation along the *y*-axis, as this deformation would entail a considerably higher energy penalty. This scenario indeed appears as the strong interaction limit of general theoretical studies on anisotropic inclusions[36,37] and justifies our neglect of the Gaussian modulus. As is well known, upon applying eq 1, the curvature c is to be measured with respect to the so-called neutral surface[38] at which area stretching and curvature deformations decouple. For a mirror-symmetric membrane, this surface coincides with the midplane of the bilayer. If peptides are associated with only one monolayer (leaving the apposed monolayer peptide-free), the membrane is no longer mirror-symmetric and the neutral surface does not necessarily coincide with the midplane. However, we shall consider strong interactions between the lipid headgroups such that variations in the cross-sectional area per lipid headgroup are energetically much more costly than any curvature deformation at the equilibrium membrane thickness (see Figure 5 and its discussion), and therefore the cross-sectional area per headgroup remains essentially fixed during a bending deformation. In this limit and for conserved membrane volume, the neutral surface coincides with the membrane's midplane as shown in the appendix.

Using the chain packing theory, we calculate the free energy per unit cell F as a function of the curvature c. To this end we consider a (possibly bent) unit cell as shown in Figure 3. (Note that we define c to be positive if the peptide-containing leaflet bends away from the peptide as illustrated in Figure 3.) The central quantity of the chain packing theory is the joint probability $P(\mathbf{r}, \alpha)$ to find a lipid chain anchored at position $\mathbf{r}$ on the membrane's polar−apolar interface, $\mathcal{M}$ (see Figure 3), and in a given conformation, α. Note the normalization $(1/A)\int_{\mathcal{M}} d^2\mathbf{r} \sum_\alpha P(\mathbf{r},\alpha) = 1$ where $A = \int_{\mathcal{M}} d^2\mathbf{r}$ is the total lipid-accessible interfacial area per unit cell. The summation over α runs over all accessible lipid conformations, that is, all those conformations retaining all chain segments inside the fluidlike hydrocarbon core and not penetrating into the rigid cylinder that represents

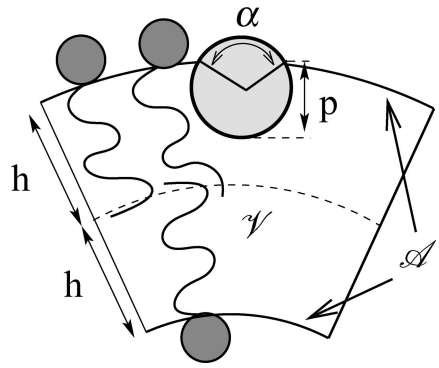

Figure 3. Cross-section of the unit cell with a number of lipids shown schematically. The membrane is bent with positive curvature c; its midplane (where the curvature is measured) is shown as a broken line. The thickness of the hydrophobic region is $2h$. The peptide resides in the upper monolayer (shaded circular region); the angle α of its hydrophilic face determines the insertion depth p. The lipid chain region and the polar−apolar interface between lipid chains and headgroups are denoted by $\mathcal{V}$ and $\mathcal{A}$, respectively. Note that the peptide is excluded from both $\mathcal{V}$ and $\mathcal{A}$.

the peptide. We note that $P(\mathbf{r}, \alpha)$ defines the local surface density of lipid headgroups at position $\mathbf{r}$ via the relation $\sigma(\mathbf{r}) = \bar{\sigma}\sum_\alpha P(\mathbf{r}, \alpha)$, where $\bar{\sigma} = N/A$ is the average headgroup density in the unit cell. In terms of $P(\mathbf{r}, \alpha)$, the mean-field expression for the conformational free energy is

$$F = \frac{N}{A}\int_{\mathcal{A}} d^2\mathbf{r}\sum_\alpha P(\mathbf{r}, \alpha)[\varepsilon(\alpha) + k_BT \ln P(\mathbf{r}, \alpha)] \qquad (2)$$

where $\varepsilon(\alpha)$ denotes the internal (trans-gauge isomerization) energy of a chain in conformation α, and k_BT is the thermal energy.

To derive an explicit expression for the equilibrium value of $P(\mathbf{r}, \alpha)$, namely the one which minimizes F, we make one simplifying approximation, that is, we assume that the density of lipid chain segments is uniform (and liquidlike) throughout the volume $\mathcal{V}$ of the hydrophobic core.[39] The uniform density assumption imposes the following chain packing constraint

$$\bar{\phi} = \frac{1}{A}\int_{\mathcal{A}} d^2\mathbf{r}\sum_\alpha P(\mathbf{r}, \alpha)\phi(\alpha, \mathbf{r}', \mathbf{r}) \qquad (3)$$

Here, $\phi(\alpha, \mathbf{r}', \mathbf{r})$ is the number of chain segments that a chain anchored at position $\mathbf{r}'$ on $\mathcal{A}$ and residing in conformation α contributes to a volume element located at $\mathbf{r}$ in $\mathcal{V}$. The requirement of a uniform packing density everywhere in $\mathcal{V}$ is expressed by the fact that $\bar{\phi} = 1/(N\nu)$ in eq 3 is a constant independent of $\mathbf{r}'$; where ν is the volume per lipid chain. The variation in $P(\mathbf{r}, \alpha)$ associated with the minimization of F corresponds, physically, to variations in the conformational properties (statistical weights of the α's) and spatial distribution of chain origins $\mathbf{r}$) along the interfacial area $\mathcal{A}$.

Minimization of F subject to the uniform density constraint leads to the equilibrium probability distribution $P(\mathbf{r}, \alpha) = \chi(\mathbf{r}, \alpha)/q$ where $q = (1/A)\int_{\mathcal{A}} d^2\mathbf{r}\sum_\alpha \chi(\mathbf{r}, \alpha)$ is the partition sum and

$$\chi(\mathbf{r}, \alpha) = \exp\left\{-\frac{1}{k_BT}\left[\varepsilon(\alpha) + \int_{\mathcal{V}} d^3\mathbf{r}\lambda(\mathbf{r})\phi(\alpha, \mathbf{r}', \mathbf{r})\right]\right\} \qquad (4)$$

is a generalized Boltzmann weight (analogous to that of the isothermal−isobaric ensemble). In eq 4, $\lambda(\mathbf{r})$ is a Lagrangian multiplier function that reflects the local lateral pressure[26] and can be determined numerically (after choosing an appropriate molecular chain model; see below) such that eq 3 is fulfilled. More specifically, insertion of the equilibrium probability distribution $P(\mathbf{r}, \alpha)$ into the constraint of uniform packing density, eq 3, results in a self-consistency relation for $\lambda(\mathbf{r})$ that can be solved numerically. Note that we do not impose any constraint other than that expressed by eq 3. Thus, we allow the lipids to freely distribute in the plane of the membrane and to move from one layer to the other so as to minimize the free energy F.[18] This is appropriate for cases in which the lipids can migrate from one layer to the other as has been reported for peptide−membrane systems.[40–42] In principle, additional constraints regarding the conservation of the number of lipids in each monolayer can be implemented as discussed in ref 29; these however are beyond the scope of the present work.

Substituting the result for $P(\mathbf{r}, \alpha)$ back into eq 2 yields our final expression for the free energy F per unit cell

$$\frac{F}{N} = -k_BT \ln q - \bar{\phi}\int_{\mathcal{V}} d^3\mathbf{r}\lambda(\mathbf{r}) \qquad (5)$$

This expression is valid for any imposed membrane curvature c and penetration depth p of the peptide. Thus, in principle, $F = F(c, p, h)$ in eq 5 fully defines the curvature elastic properties (expressed by κ and c_0) of the peptide-dressed membrane. One way to calculate the curvature dependence of $F(c, p, h)$ is to carry out systematic chain packing calculations for membranes with different curvatures. These calculations are rather involved and computationally costly. An alternative, more elegant approach is to analytically express κ and c_0 in terms of properties of the flat membrane (see eq 1) and then to use these expressions in a single chain packing calculation for a flat membrane. This approach was first introduced by Szleifer et al.[29] and is here generalized to include the presence of rigid membrane inclusions. To this end, we decompose the total lipid-accessible interfacial surface per unit cell $\mathcal{A} = \mathcal{A}_E + \mathcal{A}_I$ into contributions from the outer, peptide-containing, monolayer ($\mathcal{A}_E$ with surface area A_E) and from the inner, bare, monolayer ($\mathcal{A}_I$ with surface area A_I). We then define a measure for the asymmetry in headgroup density $S_{hg}(c) = [\bar{\sigma}_E(c) - \bar{\sigma}_I(c)]/\bar{\sigma}$ where

$$\bar{\sigma}_E(c) = \frac{1}{A_E}\int_{\mathcal{A}_E} d^2\mathbf{r}\,\sigma_E(\mathbf{r}), \qquad \bar{\sigma}_I(c) = \frac{1}{A_I}\int_{\mathcal{A}_I} d^2\mathbf{r}\,\sigma_I(\mathbf{r}) \quad (6)$$

are the average headgroup densities in the outer and inner monolayers, respectively. With this definition we obtain, after an expansion of F up to quadratic order in curvature c and comparing to eq 1

$$\kappa a_0 = k_BT\left(\frac{hS_{hg}(0)}{2 - \xi_P}\right)^2 + \frac{1}{k_BT}\int_{\mathcal{V}} d^3\mathbf{r}'\int_{\mathcal{V}} d^3\mathbf{r}''\int_{\mathcal{A}} d^2\mathbf{r}\sum_\alpha P(\mathbf{r}, \alpha)\times$$
$$\left\{\left(\frac{\partial\lambda(r')}{\partial c}\right)_{c=0} \times \left(\frac{\partial\lambda(\mathbf{r}'')}{\partial c}\right)_{c=0}[\phi(\alpha, \mathbf{r}', \mathbf{r}) - \bar{\phi}] \times [\phi(\alpha, \mathbf{r}'', \mathbf{r}) - \bar{\phi}]\right\} \quad (7)$$

where ξ_P is the area fraction of the peptide within the outer monolayer of the flat membrane. Furthermore, we obtain

$$\kappa c_0 a_0 = k_BT\left(\frac{hS_{hg}(0)}{2 - \xi_P}\right) + \int_{\mathcal{V}} d^3\mathbf{r}\lambda(\mathbf{r})\,\mathbf{r}\cdot\mathbf{n} \qquad (8)$$

where $\mathbf{n}$ is the unit vector in normal direction of the flat membrane (that is, along the z-axis in Figure 2A). The derivatives with respect to curvature are evaluated for a flat membrane ($c = 0$) as in eq 1. Thus, no explicit bending is needed to numerically determine the curvature elastic properties

TABLE 1: Equilibrium Membrane Thickness $2h_{eq}$ and Free Energy Gain upon Membrane Thickness Adjustment Per Unit Cell, ΔF_{tot} (Expressed in Units of the Thermal Energy k_BT), As a Function of the Peptide's Insertion Depth p (see Figure 3)

p/Å	0	2	4	6	8	10	12
$2h_{eq}$/Å	25.5	24.0	21.7	22.3	23.3	23.4	24.6
$-\Delta F_{tot}$	0.0	1.6	26	25	19	4	1.2

of the peptide-containing membrane. Equation 7 expresses the well-known fact that the response to an external field (here, an imposed curvature deformation, from $c = c_0$ to $c = 0$), is completely determined by the equilibrium fluctuations of the corresponding system.[43]

The curvature derivatives of $\lambda(\mathbf{r})$ in eq 7 can be found by differentiating the constraint for uniform packing density, eq 3, with respect to c, yielding a self-consistency equation for $(\partial\lambda(\mathbf{r})/\partial c)_{c=0}$ that can be solved numerically.[29] We also note that the presence of the terms with $S_{hg}(c = 0)$ in eqs 7 and 8 accounts for the asymmetric headgroup densities due to the presence of the peptide. That is, for $p > 0$ the peptide perturbs the lipid chain region, inducing a lateral reorganization of the headgroups in the upper (and to a smaller extent also in the lower) monolayer. The asymmetry in headgroup density implies a curvature-dependent cost in the lipid's translational entropy and hence affects the curvature elastic properties.

The flat membrane (for which we calculate κ and c_0 according to eqs 7 and 8) is allowed to adjust its thickness in response to inserting the peptides at various depths, p, into the hydrophobic core. The corresponding equilibrium membrane thickness is denoted by $2h = 2h_{eq}(p)$. Indeed, a decrease of membrane thickness upon peptide insertion has been observed experimentally[33] and is reproduced in model calculations;[18,44] see below. Because the bending stiffness of a membrane depends sensitively on its thickness[45] we need to include this dependence in our calculations. To obtain $h_{eq}(p)$, we add to the conformational free energy in eq 2 an interfacial tension term, γA, with $\gamma = 0.12k_BT/$Å^2 being the corresponding surface tension. We note that this term affects only indirectly the curvature elastic properties, namely through the adjustment of the membrane thickness h. The tension opposes the tendency of the lipid chains to laterally expand the membrane and thus leads to a stable equilibrium state.[25]

3. Results and Discussion

We model a lipid membrane composed of saturated myristoyl chains, $CH_3-(CH_2)_{12}-CO-$ with a volume of $\nu \approx 378$ Å^3 per chain. Our numerical calculations involve the generation of all accessible chain conformations based on the rotational isomeric state model.[46] This model is a suitable discretized approximation of the rotational (trans/gauche) energy surface of methyl segments along the lipid chain.[25] The peptides are modeled as rigid cylinders of radius $R = 6$ Å and length $D = 30$ Å. The angle α subtended by their polar face (see Figure 3) dictates the penetration depth of the peptide through $p = R[1 + \cos(\alpha/2)]$. As a typical choice of a high peptide-to-lipid ratio for which the interhelical distance is of the same order as the peptide length D, we use $N = 40$, corresponding to 40 chains per unit cell. For double-tailed lipids this implies a peptide-to-lipid ratio of 1/20. This choice is motivated by recent experiments in which similar concentrations are used to mimic the physiologically active concentrations of many antimicrobial peptides.[32–34]

Consider first a peptide-free (that is $p \leq 0$), flat, symmetric bilayer that will serve as a reference system. Numerical minimization of the total free energy (conformational free energy and surface tension contribution) leads to an equilibrium thickness of the hydrocarbon core of $2h_{eq}^0 = 2h_{eq}(p = 0) = 25.5$ Å, and a corresponding cross-sectional area per chain of $\nu/h_{eq}^0 = 29.6$ Å^2, consistent with experimental findings.[47]

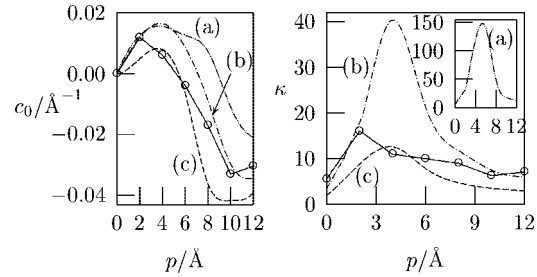

Figure 4. Spontaneous curvature c_0 (left diagram) and bending rigidity κ (measured in units of k_BT, right diagram) calculated as a function of peptide insertion depth, p, for three values of membrane thickness: $2h = 26$ Å (a), $2h = 24$ Å (b), and $2h = 22$ Å (c); open circles mark the corresponding values of the equilibrium membrane thickness $2h_{eq}(p)$. The inset displays $\kappa = \kappa(p)$ for $2h = 26$ Å, which requires a larger energy scale.

Experiment shows that the (partial) insertion of an amphipathic peptide into the bilayer's hydrophobic core results in membrane thinning that ranges between 2−4 Å.[33,48] This finding is quantitatively reproduced by our present model as demonstrated in Table 1. Table 1 lists, as a function of p, the calculated values of the equilibrium thickness $2h_{eq}(p)$ of the flat membrane, and the corresponding free energy difference, $\Delta F_{tot}(p) = F_{tot}[p,h_{eq}(p)] - F_{tot}[p,h_{eq}^0]$. The total free energy appearing here, $F_{tot} = F + \gamma A$, is the sum of chain conformational and surface energy per unit cell.

The free energy change $\Delta F_{tot}(p)$ expresses the free energy difference (per unit cell and for a given p) between a flat membrane that can optimize its thickness so as to minimize the peptide-induced membrane perturbation, and a membrane that is (artificially) constrained to maintain the equilibrium thickness h_{eq}^0 of the initial, peptide-free, state. We may thus interpret $\Delta F_{tot}(p)$ as the "relaxation free energy" of the flat membrane with respect to adjusting its thickness upon peptide insertion. For a peptide that inserts roughly half of its cylindrical body into the hydrocarbon chain region ($p \approx R = 6$ Å) the relaxation free energy is substantial, indicating a profound influence of the peptide on the energetics of the host membrane. Additional comparisons of molecular characteristics such as bond orientational order parameters of the lipid chains with available experimental data and computer simulations have been presented recently in two complementary studies of this system.[18,49]

We now turn to the main focus of the present work, that is, to the influence of peptide insertion on the curvature elasticity of the membrane as expressed by the bending stiffness κ and the spontaneous curvature c_0, according to eqs 7 and 8. Recall that for any given p, the calculation of κ and c_0 involves the properties of a flat membrane, whose well-defined equilibrium thickness is $2h_{eq}(p)$. Still, to illustrate the significance of membrane thickness adjustment we present calculations for varying membrane thicknesses.

The main results of our work are summarized in Figure 4, which shows c_0 (left diagram) and κ (right diagram) as a function of the peptide penetration depth, p, for three representative values of the membrane thickness $2h$. Also shown in both diagrams (open circles) are the corresponding values of c_0 and κ for the equilibrium membrane thickness $2h_{eq} = 2h_{eq}(p)$.

Perhaps the most notable property seen in Figure 4 (left diagram) is the change in sign of c_0, from positive to negative, as the peptide inserts deeper into the hydrophobic core. This is the quantification of the conceptual framework expressed in Figure 1. Peptides that penetrate only little into the hydrophobic core tend to bend the membrane in a positive direction (i.e., away from the peptide), whereas deeply inserted peptides induce bending in the opposite direction. These two opposite tendencies reflect conformational changes of the lipid chains in the vicinity of the peptide as will be discussed below. The change in sign of c_0 occurs roughly at $p \approx R = 6$ Å, that is, when the peptide is about halfway into the hydrophobic core.

We emphasize that the results above for the changes in elastic membrane properties due to peptide adsorption origin entirely from the perturbation of lipid chain packing in the bilayer's core. These changes may be modulated by additional energetic contributions which are not included in our model; for example, specific interactions between the peptide and lipid headgroups and in particular electrostatic interactions could influence c_0. Note, however, that the influence of the lipid chain packing is a generic feature, present for any interfacially adsorbed rigid inclusion.

Our findings, $c_0 > 0$ for $p \lesssim R$ and $c_0 < 0$ for $p \gtrsim R$, are in qualitative agreement with observations concerning class A and class L amphipathic peptides.[19] Specifically, class A peptides are characterized by a large polar angle, $\alpha > 180^\circ$, and are thus expected to insert only a small fraction of their cylinder-like bodies into the membrane. These peptides are typically found to increase the bilayer-to-hexagonal phase transition temperature, T_H, indicating the induction of positive curvature stress in the bilayer; see Figure 1, top. On the other hand, class L peptides, having a large hydrophobic face, were shown to have an opposite effect on T_H,[10,20] which is indicative of a negative curvature stress in the bilayer; see Figure 1, bottom. We note that an opposite trend has also been reported for class L peptides.[7] These apparent inconsistencies can be a reflection of additional interactions between the peptides and the membrane. For example an electrostatic repulsion between the polar faces of charged peptides would contribute to a positive curvature strain; this would then have a competing effect with that due to the lipid chains in the case of large p.

Consider now the change in the elastic free energy of a peptide-dressed membrane upon relaxing from an initially flat (and hence stressed) state ($c = 0$) to its optimal equilibrium configuration where, by definition, $c = c_0$. The corresponding gain in elastic free energy (measured per unit cell), whose magnitude is $\Delta F(p, h_{eq}, c_0) = F(p, h_{eq}, 0) - F(p, h_{eq}, c_0)$, may be referred to as the frustration energy.[24] It is given by

$$\Delta F(p, h_{eq}, c_0) = \frac{N\nu}{2h_{eq}} \kappa(p,\ h_{eq}) c_0(p,\ h_{eq})^2 \qquad (9)$$

Figure 5 shows $\Delta F(p, h_{eq}, c_0)$ as a function of p. The two branches for low and high values of p correspond, respectively, to the frustration energy resulting from a positive and negative curvature stress in the membrane. The plot reveals the amount of energy per peptide released upon optimizing the curvature of the membrane. (This interpretation is subject to a quadratic dependence of the free energy on curvature, ranging from $c = 0$ to $c = c_0$.) The frustration energy is on the order of a few k_BT, vanishing at about $p \approx R = 6$ Å where $c_0 = 0$. We note that the frustration energy may sum up to a large number for many peptides but is still small compared to the corresponding energy gain upon adjustment of the membrane thickness; see Table 1. Hence, compared to the change in membrane thickness,

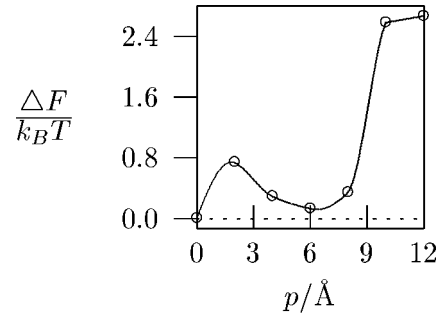

Figure 5. The free energy per unit cell associated with membrane bending from the flat ($c = 0$) to its optimal state ($c = c_0$) for which the membrane curvature is equal to the spontaneous curvature. Note that for each insertion depth, p, the membrane thickness $2h = 2h_{eq}(p)$ (see Table 1) is adjusted to its equilibrium value.

membrane curvature is a secondary effect. This conclusion reflects the strong interfacial interaction between the lipids, as assumed previously, and is in line with the elastic property of membranes in general that typically exhibit much stronger resistance to stretching as compared to bending deformations.[45]

Returning to Figure 4 (right diagram), we note the increase in κ upon peptide insertion, which is about three times larger than that of the bare membrane for ($p \approx 2$ Å) and then levels off to about 2-fold increase for larger p. Experimental evidence for peptide-induced changes of κ exist but they are scarce. It was shown, for example, that the perturbation of a lipid monolayer (on the air−water interface) induced by an antimicrobial frog peptide lead to an increased bending stiffness.[50] In another study, a number of charged farnesylated peptides were found to cause a small rigidification in a dimyristoylphosphatidylcholine bilayer.[51] A more pronounced increase in κ, 3-fold for a remarkably low peptide concentration (corresponding to $N \approx 2000$), was observed for a triblock peptide in a ternary system, containing a single-chain surfactant, water, and decane.[52,53] Taken together, our theoretical model as well as the available experimental measurements indicate that membrane rigidification is a common consequence of amphipathic peptide adsorption.

The bending stiffness of both lipid bilayers and surfactant monolayers is known to increase steeply upon increasing their thickness, reflecting the concomitant stretching, and hence lower conformational freedom of their constituent chains.[29,45] The rigidification of the peptide-dressed membrane is thus remarkable and may appear surprising because the adsorbed peptides actually lead to membrane thinning; see Table 1. While it is seemingly inconsistent that the thinner, peptide-containing, membrane has a larger bending modulus than a thicker peptide-free membrane, we note that if we hypothetically increase the thickness of the peptide-containing membrane (at constant p), κ increases as one would expect; see the right diagram in Figure 4. In the following, we argue that the increase in κ upon peptide insertion, despite membrane thinning, can be explained in terms of the changes in the conformational properties of the lipid chains surrounding the adsorbed peptide.

Figure 6 displays the cross-section of a flat, peptide-containing, membrane for two different penetration depths, $p = 10$ Å (top diagram) and $p = 4$ Å (bottom diagram). Shown in both cases are the calculated average segment positions (connected by solid lines) of lipid chains that originate at a number of arbitrarily chosen positions r on $\mathcal{M}$; the graphs on the right show the corresponding perturbation free energy per lipid chain as a function of the headgroup distance (along the x-axis) from the peptide, measured relative to the unperturbed bilayer ($p = 0$). We emphasize that the average segment

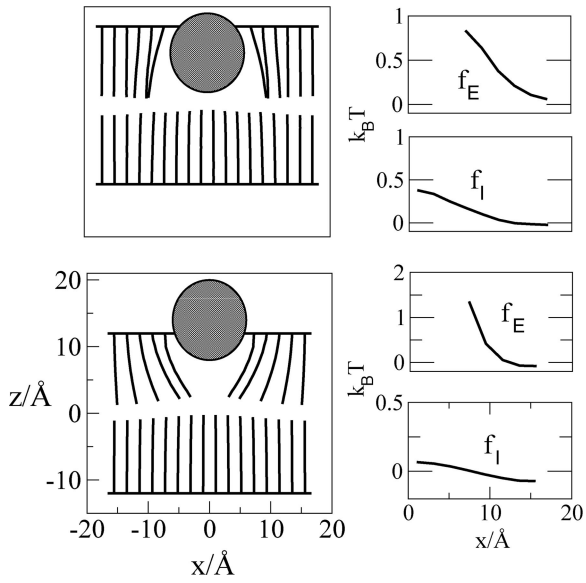

Figure 6. Conformational properties and perturbation free energy of lipid chains in a peptide-containing membrane. Left panel shows the calculated average contours of the lipid backbone for several lipid chains that originate at a number of arbitrarily chosen positions **r** on $\mathcal{A}$. The right panel shows the corresponding chain free energy of those lipids measured, per lipid, relative to the peptide-free membrane ($p = 0$); with f_E and f_I denoting the free energy of chains from the external and internal monolayers, respectively. The figure shows two representative cases of peptides penetrating into the hydrophobic core. The top diagram is calculated for $p = 10$ Å and the bottom digram for $p = 4$ Å; membrane thickness is $2h = 24$Å.

positions displayed in Figure 6 do not reflect the average segment density within the hydrocarbon core. In fact, this density is imposed to be strictly uniform; (see eq 3 and ref 18 for an analysis of the shape beyond plotting the average segment positions of the lipid chains). What the average segment positions reveal are elastic deformations such as tilt, splay, and stretching of the lipid chains due to their individual packing environments. Figure 6 is therefore helpful to qualitatively understand our two major predictions: (i) the increase in the bending rigidity of the membrane, despite the decrease in thickness, and (ii) the sign change of the spontaneous curvature.

The constraint of uniform segment density in the hydrophobic core of the membrane implies that the lipid chains have to "deform" (i.e., adjust their average conformational properties) in order to fill up (and thus prevent) the "void" otherwise created underneath the peptide. The elastic deformation of the lipids includes pronounced tilting and stretching of the chains in the peptide-containing monolayer as well as stretching of the lipids in the apposed monolayer. These elastic deformations and the associated perturbation free energy of the lipid chains are nonhomogeneous and vary along the *x*-axis; for example, the lipids originating from positions adjacent to the peptide in the same monolayer and those directly underneath the peptide are most strongly constrained to tilt and stretch toward the peptide and are thus subjected to the largest increase in the free energy per chain. The elastic lipid deformations provide the key to understand the increase in bending stiffness. That is, lipid chains underneath the peptide as well as the strongly tilted ones in the peptide-containing leaflet, are effectively stretched. The influence of these chains on the bending rigidity of the membrane is similar to that of stretched lipids in a bare membrane of larger thickness; it is these chains that account for the increase in the bending rigidity.

Figure 6 also allows us to understand the change in sign of the spontaneous curvature as a function of p. Inspection of the lipid chains belonging to the peptide-containing monolayer in the top and bottom diagrams of Figure 6 shows that these chains are tilted in opposite directions (on the average); away from the peptide region for $p = 10$ Å (top diagram) and toward the peptide region for $p = 4$ Å. The chains are also curved (to some extent) reflecting the cylindrical shape of the peptide. The opposite behaviors of the average lipid tilt explains the opposite signs of the corresponding spontaneous curvatures. The tilt away from the peptide region for large p (top diagram) is a result of the entropic repulsion of the chains from the rigid core of the (deeply inserted) peptide.[26,27,49] All chain conformations that would otherwise penetrate into the peptide are excluded and their probability is thus zero. By tilting away from the rigid core of the peptide, the lipid chains regain some of their conformational freedom. In contrast, for small p (bottom diagram), lipid chains tilt toward the peptide to fill the region underneath the peptide. In both cases the membrane may further optimize the packing of its lipids by undergoing a bending deformation away from the flat state; yet, because the energetically favored tilt of the chains is opposite for small and large p, the bending deformation will proceed in opposite directions. Hence, the spontaneous curvature has opposite sign. For an intermediate insertion depth, $p \approx R = 6$ Å, the two opposed tendencies, described above for small and large p, cancel, leading to a vanishing spontaneous curvature.

The nonmonotonic behaviors of $\kappa(p)$ and $c_0(p)$, predicted by our molecular-level chain packing calculations, are a manifestation of the complex packing characteristics of the lipid chains in the vicinity of partially inserted membrane inclusions.

4. Concluding Remarks

Our chain packing calculations provide a quantitative account of how interfacially adsorbed amphipathic peptides (of intrinsically cylinder-like shape and at large peptide-to-lipid ratio) affect the elastic behavior of the host membrane. Despite a peptide-induced thinning of the membrane we find a 2- to 3-fold increase in bending stiffness, which should be attributed to the local stretching of the chains in the vicinity of the adsorbed peptide. In addition, we find that the spontaneous curvature behaves nonmonotonically. For a small penetration depth of the peptides, the membrane bends "away" from the peptide, whereas a large penetration depth induces bending toward the peptide. The spontaneous curvature nearly vanishes when the penetration depth into the hydrocarbon core is roughly equal to the radius of the peptide.

Appendix

In this appendix, we show that the neutral surface of the peptide-containing membrane is located at the bilayer's midplane in the limit of strong interactions between the lipid headgroups. To identify the position of the neutral surface we expand the free energy per unit cell, F, in terms of both the curvature c and average cross-sectional area per lipid $a = 2A/N$, measured at the bilayer's midplane.

$$\frac{F}{A_0} = \frac{\kappa}{2}(c - c_0)^2 + \frac{K}{2}\left(\frac{a}{a_0} - 1\right)^2 + \tau c\left(\frac{a}{a_0} - 1\right) \qquad (10)$$

Reference state of the expansion is the flat ($c = 0$) and laterally relaxed ($a = a_0 = 2A_0/N$) bilayer. In eq 10, K is the lateral compressibility modulus and τ is a coupling parameter. Note that κ and c_0 correspond to the quantities defined in eq 1.

On the basis of eq 10, the position of the neutral surface is found to be located at distance $\delta = \tau/\kappa$ away from the midplane (inside the outer, peptide-containing leaflet for positive δ). The corresponding bending stiffness and spontaneous curvature, both measured with respect to the neutral surface, are then $\kappa_{ns} = \kappa(1 - 2c_0\tau/K) - \tau^2/K$ and $c_0^{ns} = c_0\kappa/\kappa_{ns}$. Hence, determination of the coupling parameter τ and lateral compressibility modulus K appears generally necessary to correctly calculate the bending stiffness and spontaneous curvature of an asymmetric lipid bilayer with reference to the midplane. Nevertheless, if a second contribution is added to F to explicitly account for strong interactions between the lipid headgroups, as assumed in the present work (together with the assumptions of fixed number N of lipids and fixed volume V of the hydrocarbon core in the unit cell) one may show that $\delta = 0$, that is, that the neutral surface coincides with the midplane and thus $\kappa_{ns} = \kappa$ and $c_0^{ns} = c_0$. The additional headgroup interaction term is written as follows:

$$F_{hg} = \int_{\mathcal{A}} d^2\mathbf{r}\, \frac{K_{hg}}{2}\left(\frac{a_i}{a_0} - 1\right)^2 \tag{11}$$

here a_i is the local cross-sectional area per lipid measured at the polar−apolar interface (a distance h from the midplane; see Figure 3); the integration runs over the entire polar−apolar interface $\mathcal{A}$ of the unit cell (accounting for both monolayers). Clearly then, the strong interaction limit between the headgroups, corresponding to $K_{hg}\to\infty$, implies $a_i = a_0$ for all lipids in the unit cell. Moreover, the cross-sectional area per lipid in the outer and inner monolayers can generally be expressed as $a_i^E = A_E/N_E$ and $a_i^I = A_I/N_I$, respectively, where $A_E = A_E^{(0)}[1 + (h - \delta)c]$ and $A_I = A_I^{(0)}[1 - (h + \delta)c]$ are the outer/inner areas of the unit cell's polar−apolar interface and $N_E = N_E^{(0)}(1 + \eta c)$ and $N_I = N_I^{(0)}(1 - \eta c)$ are the number of lipids originating in the outer/inner monolayers. In these relations $A_E^{(0)} = a_0 N_E^{(0)}$, $A_I^{(0)} = a_0 N_E^{(0)}$, $N_E^{(0)}$, and $N_I^{(0)}$ are the corresponding values for the flat membrane. The quantity $\eta c = (N_E - N_I)/N$ characterizes the curvature-dependent, asymmetry in the number of lipids between the two leaflets of the membrane; η is referred to as a relaxation parameter. On the basis of these relations, we thus find

$$a_i^E = a_0\frac{1 + (h - \delta)c}{1 + \eta c}, \qquad a_i^I = a_0\frac{1 - (h + \delta)c}{1 - \eta c} \tag{12}$$

Thus, the condition of fixed area per lipid headgroup, $a_i^E = a_i^I = a_0$, can only be fulfilled identically (for all curvatures) if $\eta = h$ and $\delta = 0$. The latter equality places the neutral surface at the midplane of the bilayer as stated above.

Finally, to provide an intuitive understanding of the interplay between the tail and headgroup interactions in the determination of the position of the neutral surface we consider a specific model that is purposely oversimplified so as to allow for a simple analytical solution. Let us assume that we model the energetics of the lipid bilayer (excluding the lipid headgroups) by the free energy (per unit area)

$$\frac{F}{A_0} = \frac{K_t}{2}\left(\frac{a_t}{a_0} - 1\right)^2 \tag{13}$$

where a_t is the cross-sectional area per lipid measured within the hydrocarbon tail region at distance h_t away from the polar−apolar interface. All bilayer interactions (excluding the headgroups) are thus assumed to take place within one single surface in each monolayer; K_t characterizes the interaction strength. To render the membrane asymmetric, we assume that K_t adopts different values in both monolayers: $K_t = K_t^E$ in the outer monolayer and $K_t = K_t^I$ in the inner monolayer. The two different interaction strengths may be considered to mimic the presence of the peptide. To F/A_0 in eq 13, we add the headgroup energy per unit area

$$\frac{F_{hg}}{A_0} = \frac{K_{hg}}{2}\left(\frac{a_i}{a_0} - 1\right)^2 \tag{14}$$

where again a_i is the cross-sectional area per lipid at the polar−apolar interface (at distance h away from the midplane). The elastic properties corresponding to $F_{tot} = F + F_{hg}$ (given in eqs 13 and 14) can easily be calculated, leading to the optimal relaxation parameter (minimizing F_{tot})

$$\eta = h - \frac{h_t}{2}\left(\frac{2K_t^E K_t^I + K_{hg}(K_t^E + K_t^I)}{(K_{hg} + K_t^E)(K_{hg} + K_t^I)}\right) \tag{15}$$

and the position of the neutral surface

$$\delta = \frac{h_t K_{hg}(K_t^I - K_t^E)}{2(K_{hg} + K_t^E)(K_{hg} + K_t^I)} \tag{16}$$

Apparently the neutral surface does generally not coincide with the midplane. For the corresponding bending stiffness, measured with respect to the neutral surface we obtain

$$\kappa_{ns} = \frac{h_t^2 K_{hg}(2K_t^E K_t^I + K_{hg}(K_t^E + K_t^I))}{(K_{hg} + K_t^E)(K_{hg} + K_t^I)} \tag{17}$$

These results are valid for any choice of K_{hg}. In the limit of strong headgroup interactions, $K_{hg}\to\infty$, eqs 15–17 read

$$\eta = h; \qquad \delta = 0; \qquad \kappa_{ns} = h_t^2(K_t^E + K_t^I) \tag{18}$$

Hence, in the limit of strong headgroup interactions the neutral surface is indeed located at the bilayer midplane and the bending stiffness $\kappa_{ns} = \kappa$ can be calculated according to eq 1 (and similarly for the spontaneous curvacture).

Acknowledgment. Financial support (S.M.) from NIH through Grant R15 GM077184 is acknowledged. A.B.S. thanks the support of the Israel Science Foundation (ISF Grant 659/06) and the U.S.−Israel Binational Science Foundation (BSF Grant 2002/075). Most of the calculations reported here were carried out at the Fritz Haber Reseach Center of the Hebrew University, which is partially supported by the Minerva Foundation, Germany.

References and Notes

(1) Farsad, K.; Ringstad, N.; Takei, K.; Floyd, S. R.; Rose, K.; Camilli, P. D. *J. Cell Biol.* **2001**, *155*, 193–200.
(2) McMahon, H. T.; Gallop, J. L. *Nature* **2005**, *438*, 590–596.
(3) Zimmerberg, J.; Kozlov, M. M. *Nat. Rev. Mol. Cell Biol.* **2006**, *7*, 9–19.
(4) Epand, R. M.; Shai, Y.; Segrest, J. P.; Anantharamaiah, G. M. *Biopolymers* **1995**, *37*, 319–338.
(5) Cornell, R. B.; Taneva, S. G. *Curr. Protein Pept. Sci.* **2006**, *7*, 539–552.
(6) Shai, Y. *Biochim. Biophys. Acta* **1999**, *1462*, 55–70.
(7) Dathe, M.; Wieprecht, T. *Biophys. Biochim. Acta.* **1999**, *1462*, 71–87.
(8) Ford, M. G. J.; Mills, I. G.; Peter, B. J.; Vallis, Y.; Praefcke, G. J. K.; Evans, P. R.; McMahon, H. T. *Nature* **2002**, *419*, 361–366.
(9) Gallop, J. L.; Jao, C. C.; Kent, H. M.; Butler, P. J. G.; Evans, P. R.; Langen, R.; McMahon, H. T. *EMBO J.* **2006**, *25*, 2898–2910.
(10) Epand, R. M. *Curr. Top. Membr.* **1997**, *44*, 237–252.
(11) Lee, S.; Furuya, T.; Kiyota, T.; Takami, N.; Murata, K.; Niidome, Y.; Bredesen, D. E.; Ellerby, H. M.; Sugihara, G. *J. Biol. Chem.* **2001**, *276*, 41224–41228.
(12) Furuya, T.; Kiyota, T.; Lee, S.; Inoue, T.; Sugihara, G.; Logvinova, A.; Goldsmith, P.; Ellerby, H. M. *Biophys. J.* **2003**, *84*, 1950–1959.

(13) Yamashita, Y.; Masum, S. M.; Tanaka, T.; Yamazaki, M. *Langmuir* **2002**, *18*, 9638–9641.
(14) White, S. H.; Wimley, W. C. *Annu. Rev. Biophys. Biomol. Struct.* **1999**, *28*, 319–365.
(15) Hristova, K.; Wimley, W. C.; Mishra, V. K.; Anantharamiah, G. M.; Segrest, J. P.; White, S. H. *J. Mol. Biol.* **1999**, *290*, 99–117.
(16) Hristova, K.; Dempsey, C. E.; White, S. H. *Biophys. J.* **2001**, *80*, 801–811.
(17) Segrest, J. P.; Loof, H. D.; Dohlman, J. G.; Brouillette, C. G.; Anantharamaiah, G. M. *Proteins* **1990**, *8*, 103–117.
(18) Zemel, A.; Ben-Shaul, A.; May, S. *Biophys. J.* **2004**, *86*, 3607–3619.
(19) Tytler, E. M.; Segrest, J. P.; Epand, R. M.; Nie, S.; Epand, R. F.; Mishra, V. K.; Venkatachalapathi, Y. V.; Anantharamaiah, G. M. *J. Biol. Chem.* **1993**, *268*, 22112–22118.
(20) Epand, R. F.; Epand, R. M.; Formaggio, F.; Crisma, M.; Wu, H.; Lehrer, R. I.; Toniolo, C. *Eur. J. Biochem.* **2001**, *268*, 703–712.
(21) Epand, R. M. *Biophys. Biochim. Acta.* **1998**, *1376*, 353–368.
(22) Nir, S.; Nieva, J. L. *Prog. Lip. Res.* **2000**, *39*, 181–206.
(23) Helfrich, W. *Z. Naturforsch.* **1973**, *28*, 693–703.
(24) Andersen, O. S.; Koeppe, R. E. *Annu. Rev. Biophys. Biomol. Struct.* **2007**, *36*, 107–130.
(25) Ben-Shaul, A. Molecular theory of chain packing, elasticity and lipid protein interaction in lipid bilayers. In *Structure and Dynamics of Membranes*; Lipowsky, R.; Sackmann, E., Eds.; Elsevier: Amsterdam, 1995; *Vol. 1*.
(26) Fattal, D. R.; Ben-Shaul, A. *Biophys. J.* **1993**, *65*, 1795–1809.
(27) May, S.; Ben-Shaul, A. *Phys. Chem. Chem. Phys.* **2000**, *2*, 4494–4502.
(28) Cantor, R. S. *J. Phys. Chem.* **1997**, *101*, 1723–1725.
(29) Szleifer, I.; Kramer, D.; Ben-Shaul, A.; Gelbart, W. M.; Safran, S. A. *J. Chem. Phys.* **1990**, *92*, 6800–6817.
(30) Brasseur, R.; Pillot, T.; Lins, L.; Vandekerckhove, J.; Rosseneu, M. *Trends Biochem. Sci.* **1997**, *22*, 167–171.
(31) Perez-Mendez, O.; Vanloo, B.; Decout, A.; Goethals, M.; Peelman, F.; Vandekerckhove, J.; Brasseur, R.; Rosseneu, M. *Eur. J. Biochem.* **1998**, *256*, 570–579.
(32) Koenig, B. W.; Ferretti, J. A.; Gawrisch, K. *Biochemistry* **1999**, *38*, 6327–6334.
(33) Ludtke, S. J.; He, K.; Huang, H. W. *Biochemistry* **1995**, *34*, 16764–16769.
(34) Bechinger, B.; Lohner, K. *Biochim. Biophys. Acta* **2006**, *1758*, 1529–1539.
(35) Dan, N.; Pincus, P.; Safran, S. A. *Langmuir* **1993**, *9*, 2768–2771.
(36) Fournier, J. B. *Phys. Rev. Lett.* **1996**, *76*, 4436–4439.
(37) Kralj-Iglic, V.; Heinrich, V.; Svetina, S.; Zeks, B. *Eur. Phys. J. B* **1999**, *10*, 5–8.
(38) Safran, S. A. *Statistical Thermodynamics of Surfaces, Interfaces and Membranes*, 1st ed.; Addison-Wesley: Reading, MA, 1994.
(39) Tanford, C. *The Hydrophobic Effect*, 2nd ed.; Wiley-Interscience: New York, 1980.
(40) Matsuzaki, K.; Murase, O.; Tokuda, H.; Fujii, N.; Miyajima, K. *Biochemistry* **1996**, *35*, 11361–11368.
(41) Uematsu, N.; Matsuzaki, K. *Biophys. J.* **2000**, *79*, 2075–2083.
(42) Li, W.; Nicol, F.; Szoka, F. C., Jr. *Adv. Drug Deliv. Rev.* **2004**, *56*, 967–985.
(43) Kubo, R. *Statistical Mechanics*, 1st ed.; North-Holland: Amsterdam, 1965.
(44) Huang, H. W.; Chen, F. Y.; Lee, M. T. *Phys. Rev. Lett.* **2004**, *92*, 198304–1.
(45) *Structure and Dynamics of Membranes*; Lipowsky, R.; Sackmann, E., Eds.; Elsevier: Amsterdam, 1995.
(46) Flory, P. J. *Statistical Mechanics of Chain Molecules*; Wiley-Interscience: New-York, 1969.
(47) Balgavý, P.; Dubniková, M.; Kuerka, N.; Kieslev, M. A.; Yaradaikin, S.; Uhríková, D. *Biophys. Biochim. Acta.* **2001**, *1512*, 40–52.
(48) Chen, F. Y.; Lee, M. T.; Huang, H. H. *Biophys. J.* **2003**, *84*, 3751–3758.
(49) Zemel, A.; Ben-Shaul, A.; May, S. *Eur. Biophys. J.* **2005**, *34*, 230–242.
(50) Konovalov, O.; O'Flaherty, S. M.; Saint-Martin, E.; Deutsch, G.; Sevcsik, E.; Lohner, K. *Physica B: Condens. Matter* **2005**, *357*, 185–189.
(51) Rowat, A. C.; Hansen, P. L.; Ipsen, J. H. *Europhys. Lett.* **2004**, *67*, 144–149.
(52) Tsapis, N.; Urbach, W.; Ober, R. *Phys. Rev. E* **2001**, *63*, 419031–419035.
(53) Tsapis, N.; Ober, R.; Chaffotte, A.; Warschawski, D. E.; Everett, J.; Kauffman, J.; Kahn, P.; Waks, M.; Urbach, W. *Langmuir* **2002**, *18*, 4384–4392.

JP711107Y